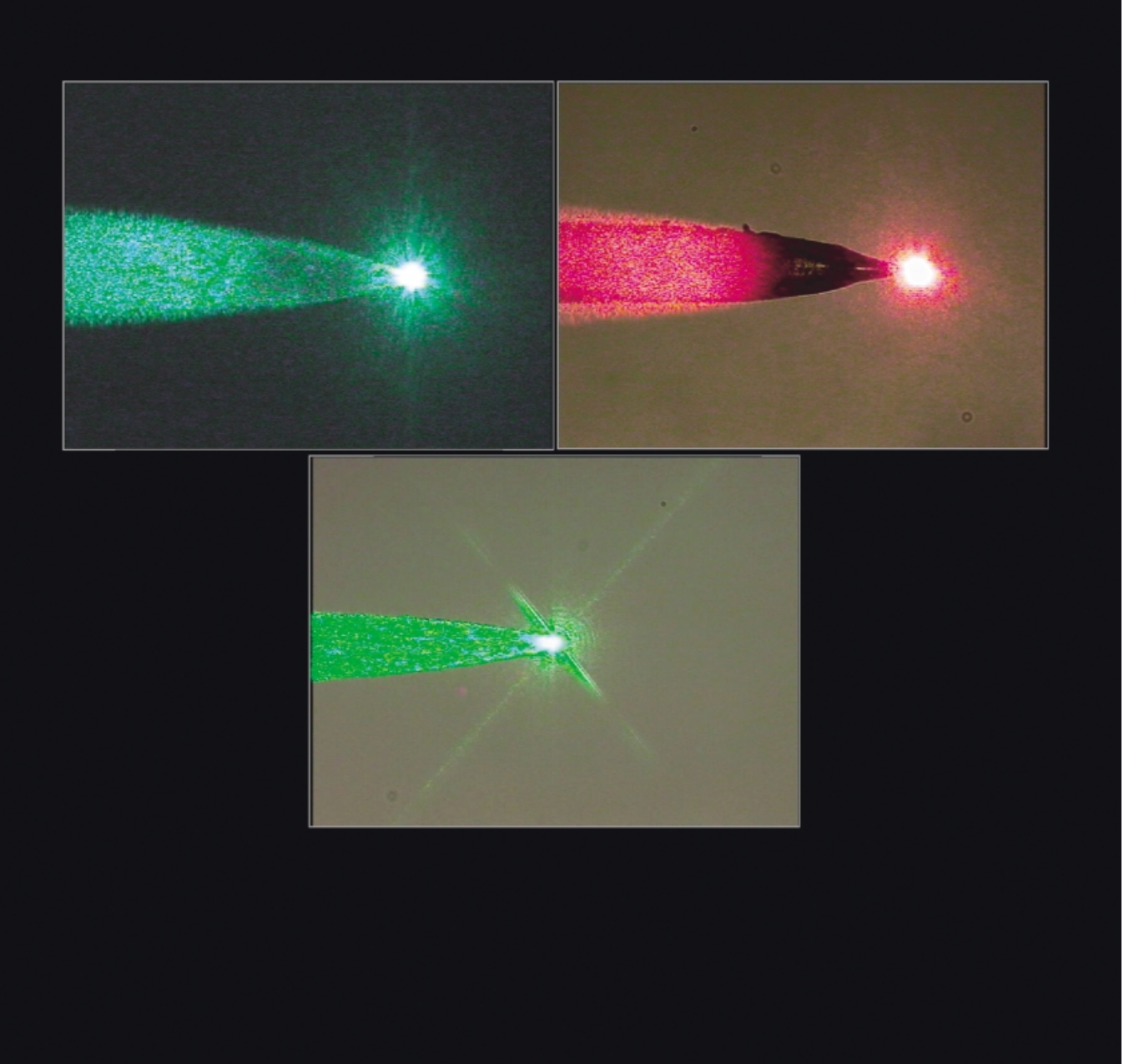
Microscopic light sources for highly sensitive Raman spectroscopy of biosamples.



Raman Spectroscopy—A Prospective Tool in the Life Sciences

Renate Petry, [a, b] Michael Schmitt, [a] and Jürgen Popp*[a, b]

Although the physics of Raman spectroscopy and its application to purely chemical problems is long established, it offers a non-invasive, nondestructive, and water-insensitive probe to problems in the life sciences. Starting from the principles of Raman spectroscopy, its advantages, and methods for signal enhancement, the bulk of the review highlights recent applications. Structural investigations of a hormone receptor, testing the

biocompatibility of dental implants, probing soil components and plant tissue alkaloids, and localization of single bacteria are just four problems in which Raman spectroscopy offers a solution or complements existing methods.

KEYWORDS:

confocal microscopy • life sciences • Raman spectroscopy • SERS • vibrational spectroscopy

Nowadays the investigation of the behavior as well as the metabolism of biomolecules on a molecular level has become central to scientific fields such as medical, pharmaceutical, and microbiological diagnostics. Understanding cellular processes is necessary for the development of new biotechnologies, medical diagnostics, and newly designed drugs, as well as in food and environmental technology. So far, standard techniques such as optical microscopy, fluorescence spectroscopy, and immunoassays have dominated the field of bioanalysis because of their high sensitivities. However, all these methods suffer from a lack of specificity and reveal only little or no molecular information. Raman spectroscopy provides information on a molecular level without labeling the biomolecule. The specificity of Raman spectroscopic techniques is extremely high, whereas the sensitivity is rather poor. Although Raman spectroscopy has been known for more than 70 years, its feasibility as a powerful method in biospectroscopy has only been repeatedly proven in the last few decades.

The number of groups active in the field underlines the potential of Raman spectroscopy as a powerful tool in biological, medical, pharmaceutical, and environmental applications. Raman spectroscopic techniques can be applied for the rapid identification of pathogenic organisms or for the early in vivo detection of cancer. Puppels and colleagues have reviewed a variety of biomedical applications, where the status of the field and the technical requirements for the clinical implementation were critically discussed. $^{[1,\,2]}$ Carey has reported on UV resonance Raman spectroscopy (UVRR), which can be used for analytical, physical, and biophysical chemistry.[3] Asher has shown the unique selectivity of the UVRR techniques that can speciate individual analytes in complex samples. [4-9] Carter and Edwards applied Raman spectroscopy for the characterization of proteins (for example wool and keratin, the latter in nails, hair, and skin) and of other biological materials (such as ivory, bone, and gallstones/kidney stones).[10] The intermolecular interactions and dynamics can be elucidated from the Raman spectrum of proteins and nucleic acids. Thomas Jr. has summarized the use of

time-resolved Raman spectroscopy, polarized Raman microspectroscopy, UVRR, and difference Raman spectroscopy, which demonstrates the potential of the various methods to determine the structural parameters in viruses or the intermolecular mechanisms that govern protein/DNA recognition in gene regulatory complexes.[11] Progress and future developments in Raman microspectroscopy and in confocal Raman microspectroscopy are outlined in reviews by Puppels, Otto, and Greve, which emphasize the potential for cell biology investigations.[12, 13] Chemical and spatial information can be obtained by established methods of Raman spectroscopy imaging of biological and biomimetic samples on a microscopic and macroscopic scale. Extrinsic labeling or staining, which might interfere with the system under investigation, is not required, thus providing a considerable advantage of this analytical tool.[14] Recent approaches in the detection of single molecules have been described by Kneipp et al. where surface-enhanced Raman scattering (SERS) was applied using nonresonant nearinfrared excitation.[15, 16] The SERS technique generally profits from the strong increase of the intrinsically weak Raman signals caused by the presence of nanosized metallic structures, for example when the target molecule is attached to colloidal silver and gold clusters. In particular, when only a small sample amount is available, surface enhancement methods offer promising opportunities in biology, medicine, and pharmacy, and allow studies of the relationships between the structure and function of proteins.[17] The evolution of Raman spectroscopic techniques in biology and medicine has been summarized

 [[]a] Prof. Dr. J. Popp, Dr. R. Petry, Dr. M. Schmitt Institut für Physikalische Chemie Universität Würzburg
 Am Hubland, 97074 Würzburg (Germany)

[[]b] Prof. Dr. J. Popp, Dr. R. Petry Institut für Physikalische Chemie Friedrich-Schiller-Universität Jena Helmholtzweg 4, 07743 Jena (Germany)

Jürgen Popp, born in 1966, received his Ph.D. in chemistry from the University of Würzburg in 1995. In 1996 he spent a year in the Department of Applied Physics of Yale University, USA. He subsequently joined the group of Prof. Dr. W. Kiefer, University of Würzburg, where he finished his habilitation in 2000; since May 2002 he has been a full professor at the University of Jena. His work has been awarded by the faculty prize of chemistry (1995), by the



Bayerischer Habilitationsförderpreis (1997), by the Förderpreis der Würzburger Korporationen (2001), and the Kirchhoff – Bunsen award (2002). His research interests are focused on biophysical systems, on the elucidation of molecular structure in biomolecules, the investigation of single microparticles, and the development of new spectroscopic measuring techniques. Since 2000 he has been an editorial board member of Journal of Raman Spectroscopy.

Renate Petry, born in 1959, has moved from engineering to the study of physics in Freiburg and Würzburg. In 1994/1995 she undertook thermodynamic investigations on inorganic systems at the Max Planck Institute of Solid State Physics, Stuttgart. From 1996 to 1999 she went for postgraduate studies to the department of biochemistry and microbiology at the University of Cape Town. Since then her interests focus on the structure – function relationships of



membrane proteins to study the ligand – receptor binding mechanisms of mammalian hormone receptors. As a Ph.D. candidate in the Kiefer group (since 1999) she was also involved in the structural characterization and analysis of helical model peptides by Raman and NMR spectroscopy. Since 2002 she has been employed by the University of Jena to continue with spectroscopic investigations in biological chemistry.

Michael Schmitt, born in 1968, received his Ph.D. in chemistry from the University of Würzburg in 1998. From 1999 to 2000 he went for postgraduate studies to the Steacie Institute for Molecular Sciences at the National Research Council of Canada. He subsequently joined Prof. Dr. W. Kiefer the University of Würzburg, where he is currently working on his habilitation. His research interests are focused on the investigation of nonadiabatic dy-



namics in polyatomic molecules on an ultrashort (femtosecond) time scale and on Raman and resonance Raman measurements of biomolecules.

comprehensively in a topical review from the research groups of Dasari and Feld.^[18] The authors have presented examples of real-time diagnosis of disease and in situ evaluation of living tissue as well as long-term directions for future studies. The theory and the measurement of Raman optical activity (ROA) of biological molecules has been described by Nafie, Barron, and co-workers.^[19–22] Puppels has recently reviewed medical applications of Raman spectroscopy^[23] and further applications in life, pharmaceutical, and natural sciences can be found elsewhere.^[24]

The intention of this Review is to present an overview in the expanding field of Raman biospectroscopy and about various Raman spectroscopic applications. We will focus on numerous ways of enhancing the sensitivity of Raman spectroscopy and on some key developments in Raman instrumentation. We will focus mainly on our work in the field of Raman spectroscopy in the life sciences.

General Aspects of Raman Spectroscopy

Spontaneous Raman Scattering

When light is incident on matter (for example on a biological cell, tissue, or micro-organism) it can interact with the atoms or molecules in several ways. Photons can be absorbed directly or can be scattered. Absorption of light is most likely if the wavelength of the radiation is in the infrared (IR) or in the ultraviolet (UV). The IR absorption results in the excitation of vibrational modes of the molecules, while the UV absorption results in the excitation of an electronic transition which is often followed by a radiative emission, fluorescence.^[25] In Figure 1 the mechanisms of fluorescence and IR absorption are shown.

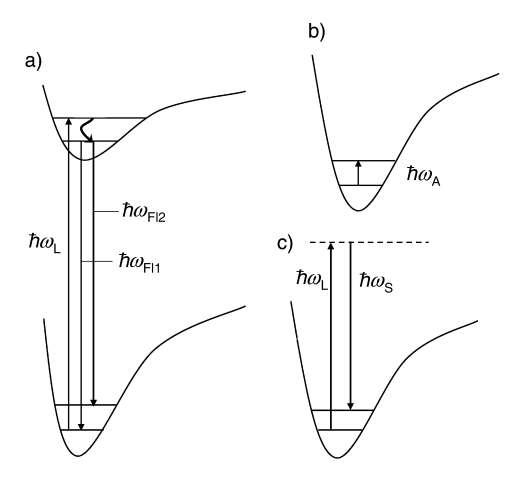


Figure 1. Simple model illustrating a) fluorescence, b) IR absorption, and c) Raman scattering. $\omega_L =$ laser frequency, ω_{FII} , $\omega_{\text{FIZ}} =$ frequency 1,2 (fluorescence); $\omega_A =$ absorption frequency; $\omega_S =$ frequency of Stokes scattered light.

When light is scattered from a molecule most photons are elastically scattered. The scattered photons have the same energy (wavelength) as the incident photons. However, a small fraction of light (approximately 1 out of 10⁸ photons) is scattered at optical frequencies different from the frequency of the incident photons. The process leading to inelastic scattering is

called the Raman effect. An energy transfer occurs as a result of the coupling between the incident radiation and the quantized states of the scattering system (schematically depicted in Figure 1c). Depending on the coupling, the incident photons either lose (Stokes) or gain (anti-Stokes) energy on the vibrational – rotational or electronic level.[82] The scattered light with lower energy as compared to the incident laser light is called Stokes - Raman scattering and the radiation with higher energy is referred to as anti-Stokes - Raman scattering. In Figure 2 a simple model of the inelastic light scattering mechanism is depicted. A photon of energy $\hbar\omega_1^{[*]}$ is incident on the scattering wavelength for the Raman process in the near-infrared (NIR) region (see "Raman Techniques and Instrumentation") or by applying special techniques such as surface-enhanced Raman scattering (see "Raman Signal Enhancement").

Raman Signal Enhancement

The classical spontaneous Raman scattering is a powerful analytical tool allowing the investigation of the qualitative as well as the quantitative composition of biological samples. However, there are serious drawbacks involved with spectro-

scopic studies based on spontaneous

Raman scattering: First, the conversion efficiency of the Raman effect is fairly poor. Only a small amount, 10^{-6} to 10^{-8} , of the laser photons is converted into Raman photons, limiting the detection of molecules for example in cells or tissue with very low concentration. Second, certain molecular systems (such as fluorophores) exhibit high fluorescence quantum yields and even weak fluorescence signals may be strong enough to mask the Raman signals. Both facts often hinder the recording of Raman spectra from biological samples. To circumvent the above-mentioned problems, special Raman techniques can be applied. The following subsections will deal with two approaches, namely the resonance

Raman effect (RRE) and surface-enhanced Raman scattering (SERS), which can enhance the intensity of Raman signals by several orders of magnitude and can quench the fluorescence. Both effects are essential when dealing with biomolecules or biological samples.

Resonance Raman Effect (RRE)

Raman spectroscopy is typically performed with excitation from green, red, or near-infrared lasers. The wavelengths are below the first electronic transitions of most molecules. As a matter of fact, being far away from an electronic absorption will avoid the excitation of fluorescence. However, there are also some advantages if the wavelength of the exciting laser lies within the electronic spectrum of a molecule. Certain substances have the ability to scatter the laser radiation with strongly increased intensity (up to 10⁶ times stronger than normal Raman scattering) if the excitation frequency of the laser is close to the frequency required for an electronic excitation. Resonance enhancement does not begin at a sharply defined wavelength. Two types of resonance Raman effects can be distinguished: the preresonance effect (pre-RRE) and the rigorous resonance effect (RRE). In most cases, the closer the excitation energy approaches the electronic resonance condition, the greater the intensity of the observed Raman bands. In Figure 3 the conventional Raman effect, the pre-RRE, and the RRE are depicted.

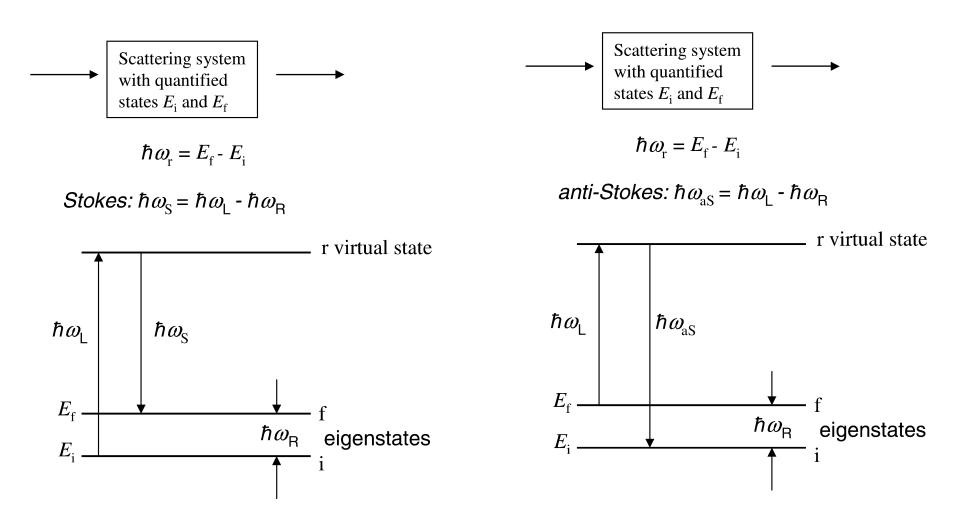


Figure 2. Model for the illustration of Stokes – Raman and anti-Stokes – Raman scatterina

system with the energy level $\hbar\omega_R = E_f - E_i$, where i and f denote two quantum states. The Stokes-Raman effect results from a transition from the lower energy level (E_i) to a higher one (E_f) . The anti-Stokes effect transfers energy from the system to the incident light wave, which corresponds to a transition from a higher energy level (E_f) to a lower one (E_i) . The anti-Stokes intensity is less than the Stokes intensity because the anti-Stokes scattering occurs from an excited state (E_f) , which is, according to the Boltzmann distribution, less populated than the ground state (E_i) . Hence, in most cases the more intense lines of the Stokes - Raman spectrum are detected. Raman scattering can occur due to changes in vibrational, rotational, or electronic energy of a molecule. Physical biochemists are concerned primarily with the vibrational Raman effect. In the following we will therefore use the term Raman effect to mean the vibrational Raman effect only. The observation of Raman scattering is in some cases limited by the excitation of fluorescence, which is typically exhibits an intensity that is several orders of magnitude stronger than Raman scattering. This phenomenon is essential in investigations of biomolecules or biological systems because they often contain fluorophores, which fluoresce when excited with light in the visible range. However, this problem can be solved by using an excitation

^[*] To clarify notation, $h\nu \equiv \hbar\omega$.

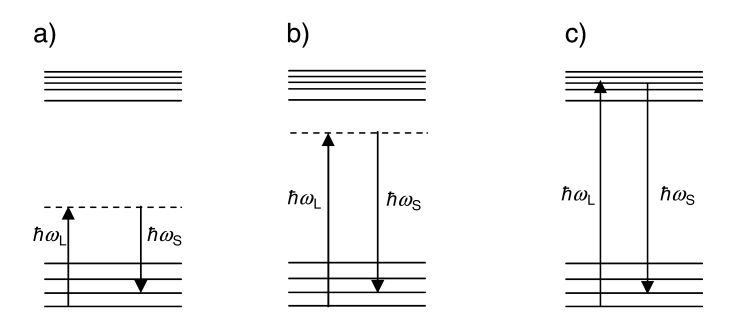


Figure 3. Energy diagram for a) the conventional Raman effect, b) the preresonance Raman effect, and c) the rigorous resonance Raman effect.

In addition the selection rules also change and only certain vibrational transitions are selectively enhanced. Higher order transitions (overtones and combination bands), which normally do not show up in conventional Raman scattering, are often visible under resonance Raman scattering conditions.[26] This effect gives rise to new bands, and therefore additional information can be deduced from a resonance Raman (RR) spectrum. Resonance Raman spectroscopy is of great interest in the case of large polyatomic molecules, such as biological molecules, where the absorption is often localized in a particular group of a large molecule, the so-called chromophore. The RR enhancement permits the isolation of the Raman bands belonging to this chromophore and structural units located close to it. This allows the physical biochemist to probe the chromophoric site (often the active site) without spectral interference from the surrounding environment (for example proteins). The change in the selection rules as well as the enhancement of specific vibrational transitions by up to six orders of magnitude give rise to various application of both preresonance Raman spectroscopy (pre-RRS) and resonance Raman spectroscopy (RRS) in physics, chemistry, biochemistry, as well as in biology. For utilizing the RRE no special equipment, other than used for conventional Raman spectroscopy, is necessary. However, it may be suitable to use a tunable laser as excitation source, which allows an appropriate adjustment of the excitation energy lying in the electronic absorption. Since many molecules absorb in the ultraviolet, the high costs of lasers and optics for this spectral region has limited UV resonance Raman spectroscopy to a small number of specialists. For more information on resonance Raman spectroscopy, refer to ref. [27].

Surface-Enhanced Raman Scattering (SERS)

The effect of drastically enhanced Raman signals from molecules adsorbed on an electrochemically roughened silver surface was discovered by Fleischmann et al.^[28] Due to electromagnetic and chemical enhancement factors a Raman signal increase by up to six orders or even more of magnitude can be observed. The first is an enhanced electromagnetic field produced at the surface of the metal. When the wavelength of the incident light is close to a surface plasmon resonance (collective excitation of conductive electrons in small metallic structures) molecules adsorbed or in close proximity to the surface experience an exceptionally large

electromagnetic field. The second mode of enhancement, also known as the chemical enhancement, is due to a charge transfer interaction between the metal and adsorbed molecules. The electronic transitions of many charge transfer complexes are in the visible region, so that resonance enhancement occurs.

The selection rules for SERS are essentially the same as those for conventional Raman spectroscopy. In particular, because the strength of the local electromagnetic field at the surface has its maximum in the direction normal to the surface, vibrational modes arising from changes in the polarizability of the adsorbate that are perpendicular to the surface will be preferentially enhanced (for details see Creighton,^[29] or Moskovits,^[30, 31] and references therein). The normal direction of the electromagnetic field, in combination with the fact that the electromagnetic amplitude strongly decreases with the distance from the surface, allows one to determine the adsorbate's orientation with respect to the average surface normal. Furthermore, information about the proximity of the adsorbate functional groups to the surface can be deduced.

A SERS experiment basically consists of the same components as applied for conventional Raman spectroscopy. In order to optimize the electromagnetic surface-enhancement effect, the laser frequency used has to match the frequency of a plasmon resonance. Since the enhancement effect strongly depends on the physical properties of the substrate, different types of substrates have been used. The most common nanostructured substrates are electrodes, sols, metal films, and silver metal island films.[32] Because SERS provides both rich spectroscopic information and high sensitivity as a result of the large enhancement effect, it is ideally suited for trace analysis. SERS allows an easy observation of Raman spectra from solution concentrations in the micromolecular range. Even further efforts were made for the detection of single molecules by means of SERS.[33-35] The method has been applied for the study of a variety of molecules of biological importance. Recently, other metals, such as copper or gold, also showed enhanced Raman spectra under certain conditions. For more information we refer the interested reader to refs. [15, 27, 36].

Raman Techniques and Instrumentation

Instrumentation

Most important for Raman biospectroscopy is the appropriate choice of the excitation wavelength of the laser. For analytical linear Raman spectroscopy mostly continuous wave (cw) lasers with a fixed wavelength are applied. In the last two decades argon and krypton ion lasers were used in many Raman laboratories. Due to the development of very sensitive micro-Raman setups nowadays He – Ne lasers are also in use as a light source for Raman spectroscopy. Recently, red diode lasers operating at 785, 810, or 830 nm as well as cw Nd:YAG lasers (1064 nm) have been used in Raman spectroscopy. In particular the development of those NIR lasers, which often avoid the excitation of Raman-masking fluorescence, has stimulated the field of biospectroscopy.^[37] For resonance Raman investigations

REVIEWS

laser lines in the ultraviolet are often necessary. The UV lines may be provided by an argon ion laser (at 275, 300, 305, 333, 351, and 363 nm, or the frequency-doubled lines at 244 and 257 nm) or pulsed laser systems such as the third (at 355 nm) and fourth harmonic output (at 266 nm) of a Nd:YAG laser.

Two different Raman spectrometers are usually applied for Raman biospectroscopy, either a dispersive one or a Fourier transform (FT) spectrometer. Nowadays the standard configuration for a dispersive spectrometer is either a triple monochromator or a single monochromator in combination with sharp-cut filters, such as a multilayer dielectric interference filter or a diffraction filter. In a triple monochromator the first two stages (substractive mode) are used for the elimination of the Rayleigh scattered light, whereas the third monochromator, the so-called spectrograph, disperses the collected Raman radiation onto a multichannel detector. Thus the Raman spectra can be recorded very close (within a few wavenumbers) to the Rayleigh line. However this has to be paid for by the poor transmittance of light. Otherwise, in case one is interested in a high light throughput and collection efficiency rather than in the recording of low frequency modes close to the Rayleigh line, the appropriate choice will be a single grating monochromator in combination with a notch filter. The detection of the Ramanscattered light is typically achieved by the application of multichannel detector devices. The most common multichannel detectors consist of either intensified diode arrays or chargecoupled devices (CCD). Both detectors possess the multiplex advantage, which allows for simultaneous detection of a large spectral range.

Excitation in the near-IR (cw Nd:YAG laser, 1064 nm) in combination with a FT spectrometer reduces the problems of fluorescence, thermal, and photochemical decomposition. Furthermore, the use of interferometric optics gives rise to achieving multiplex measurements, partially compensating the ω^4 dependence of the signal intensity. Pioneering work in FT-Raman spectroscopy has been performed by Hirschfeld and Chase^[38, 39] in 1986 and several other groups have contributed to this field. [25, 40] Usually, a fast Fourier transform (FFT) algorithm transforms the interferogram into a power density spectrum. The resolution of a FT-Raman spectrum depends on the traveling distance x of the moving mirror and on the apodization factor used in transforming the spectrum. In a FT-Raman setup the entrance slit is replaced by a spherical pinhole causing a much higher light throughput (Jacquinot advantage^[25]) than possible in a conventional dispersive Raman spectrometer. The detection is performed by a liquid nitrogen-cooled germanium detector or by an InGaAs detector, which can be operated at room temperature.

Raman measurements of liquids and solids usually do not require special sample preparation. If the measurements are performed in the visible excitation range ordinary glass sample cells can be used. Also, substances dissolved in water can be investigated in glass cells by Raman spectroscopy without any further preparation, because water as well as glass reveals only very weak Raman signals. However, if resonance Raman experiments are done in the UV, glass sample cells need to be replaced by quartz ones.

Special attention has to be paid for light-absorbing samples in order to avoid thermal decomposition. Therefore, Kiefer and coworkers have developed several experimental arrangements for the investigation of light-sensitive solids as well as liquids using rotating cell techniques.^[41–43]

Special Techniques in Raman Spectroscopy: Micro-Raman and Confocal Micro-Raman Spectroscopy

Nowadays the micro-Raman technique is a well established method for both the investigation of samples in the order of picograms or even less and the spectroscopic imaging of sample surfaces. [44, 45] A typical micro-Raman setup is displayed in Figure 4. A microscope objective serves to focus the laser beam

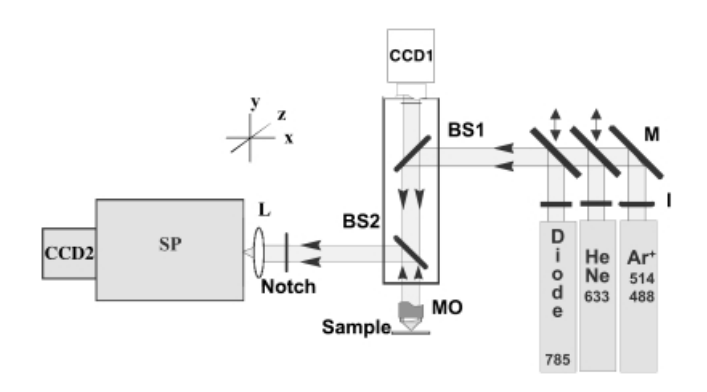


Figure 4. Schematic of a micro-Raman setup featuring different types of laser for the excitation; interference filter I; mirror M; beam splitters BS1 and BS2; microscope objective MO; camera for sample observation CCD1; lens L; spectrometer SP; optical multichannel array OMA; Peltier-cooled camera for recording of the spectra CCD2.

on the sample and to collect the scattered light. Microscope objectives with a high numerical aperture and high magnification are used to focus the light down to the diffraction limit. The 514 nm line of an argon ion laser can be focused to a spot size of about $1\,\mu\text{m}^2$. Since in many cases the focused laser spot produces high power densities, typically in the range between 10^4 to 10^6 W cm $^{-2}$, various techniques for Raman spectroscopy of microscopic samples have been developed (such as the rotating sample technique $^{[46]}$ or surface scanning Raman microscopy $^{[47]}$) in order to avoid heating and decomposition of sensitive samples, especially absorbing biological samples. For the investigation of fluorescent microsamples such as dyes or biological cells the FT-Raman spectroscopy with long-wavelength excitation is also available in combination with a microscope.

In order to obtain spatially resolved information from the sample, Raman mapping or imaging can be used. [45, 48, 49] A major problem with many micro-Raman studies is that of obtaining a good spatial resolution perpendicular to the optical axis (lateral) as well as along the optical axis of the microscope. In a conventional microscope, the entire field of view is uniformly illuminated and observed. With a confocal arrangement the resolution along the optical axis can be increased. Confocal microscopy uses a pinhole, which isolates the light originating from a small region of the sample coincident with the

illuminated spot. This simultaneously eliminates the contributions from the out-of-focus zones efficiently. [50-54] Thus, the advantage of spatial filtering by an optically conjugated pinhole diaphragm is achieved (Figure 5). Mostly a physical aperture such as an adjustable pinhole is applied. However, similar results can be obtained by using a CCD detector as a quasi "electronic" aperture. The confocal aperture is designed to collect the Raman radiation that originates only from a laser focal volume within the diffraction limit. Using high objectives (NA = 0.90 – 0.95) allows one to obtain a focal tube with a waist diameter of 1.22 λ / NA and a depth 4λ /(NA)². [55, 56]

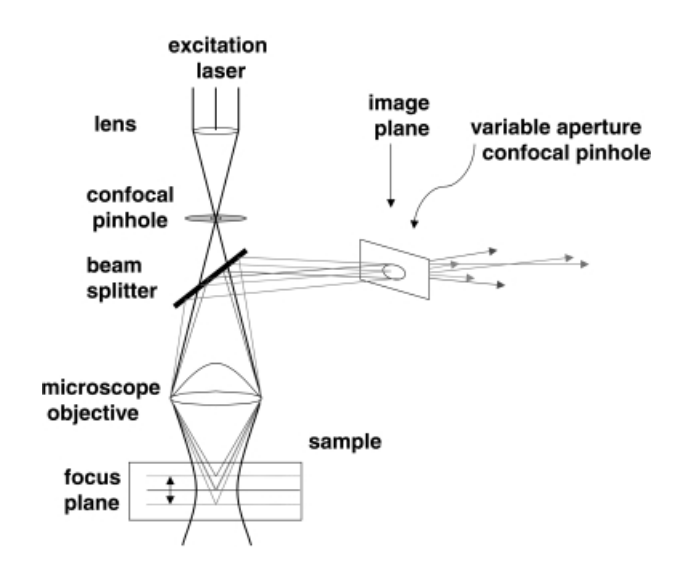


Figure 5. Schematic of confocal micro-Raman spectroscopy.

Applications

Raman biospectroscopy provides information on the structure and on intramolecular and intermolecular interactions. The recording of a Raman spectrum often requires small sample amounts and hardly any sample preparation, and unlike IR spectroscopy, water can be readily used as a solvent. However, biological systems are prone to fluorescence and other effects (such as thermal decomposition or organic impurities), which may deteriorate or even completely mask a spectrum. It is noteworthy that the choice of a suitable investigation method is never straightforward, but rather requires one to work around these drawbacks. For each biological system the most appropriate instrumentation, excitation source, and sample preparation needs to be found. The following section will present a range of applications performed in our laboratories that demonstrates the power of Raman spectroscopy in the life sciences.

Environmental, Pharmaceutical, and Medical Research

Structural Investigations on Hormone Receptors

The spectroscopic study of biomembrane structure is a complex topic, challenging a variety of physico-chemical methods such as X-ray diffraction, NMR, ESR, neutron and Raman scattering, differential scanning calorimetry, and electron cryomicroscopy.

Particular care has to be taken when structural assumptions on membrane proteins are deduced exclusively from Raman data.

The third extracellular loop (ECL3) of the gonadotropin-releasing hormone (GnRH) receptor has been studied by micro-Raman and FT-Raman spectroscopy as a complement to circular dichroism (CD) and 2D NMR spectroscopy. [57] The hormone receptor consists of seven hydrophobic (α-helical) transmembrane domains, and extramembraneous loops, thus exhibiting a high level of structural homology in the family of rhodopsin-like G protein-coupled receptors (GPCR). [58] Molecular models of the GPCR family have been based on structural data obtained from X-ray crystallography of bacteriorhodopsin [59] and of bovine rhodopsin. [60] Structural information on the transmembrane domains and the loops can be pieced together to generate a molecular model of rhodopsin and related GPCRs including the GnRH receptor that allows prediction of how GnRH binds and activates its receptor. [61, 62]

The receptor interacts with GnRH, a hypothalamic decapeptide, which regulates the release of luteinizing hormone, follicle stimulating hormone, and ultimately steroidogenesis and gametogenesis. Studies on GnRH and on the GnRH receptor provide profound pharmaceutical potential in the treatment of infertility, hormonal contraception, and applications in medical therapy to treat prostate cancer.^[63]

The loop contains an acidic amino acid that confers agonist selectivity for arginine (Arg8) in mammalian GnRH. It was proposed that a specific conformation of ECL3 is necessary to orientate the carboxyl side chain of the acidic residue for interaction with Arg⁸ of GnRH.^[64] To probe the structural contribution of the loop domain to the proposed presentation of the carboxyl side chain, a model peptide was synthesized by conventional solid-phase peptide synthesis using tBOC chemistry. The sequence represented the residues 293 – 302 of mouse ECL3 (CGPEMLNRVSEPGC), where Cys and Gly residues were added symmetrically at the N and C termini, which allowed the introduction of a disulfide bridge to simulate the distances at which the ECL3 is tethered to the transmembrane domains 6 and 7 of the receptor. The synthetic peptide could thus be studied in the linear, unconstrained conformation and also in the looplike cyclic form, as present in the native receptor (Figure 6). The disulfide bond in the cyclic peptide was produced by air oxidation of the linear peptide for 12 h, followed by HPLC purification. Mass spectrometry (MALDI-TOF) was performed subsequently and confirmed the calculated molecular weight of the cyclic and of the linear peptide. Excitation in the visible (514 nm) and in the NIR (1064 nm) range was employed, and from the consistency and reproducibility of the obtained micro-Raman and FT-Raman spectra it was assumed that the conformation of the peptides was unaffected, even after long exposure to the laser beam. The vibrational modes of the peptide backbone exhibited characteristic bands (amide III and I), which reflect on the conformation present in the linear and in the cyclic loop (Figure 7). The structure-sensitive, strong amide I band originates mainly from carbonyl C=O stretching vibrations and minor contributions of coupled vibrations of C-N stretching and N-H in-plane bending. For both ECL3 peptides, in the cyclic and in the linear form, the wavenumbers of the amide I band

REVIEWS

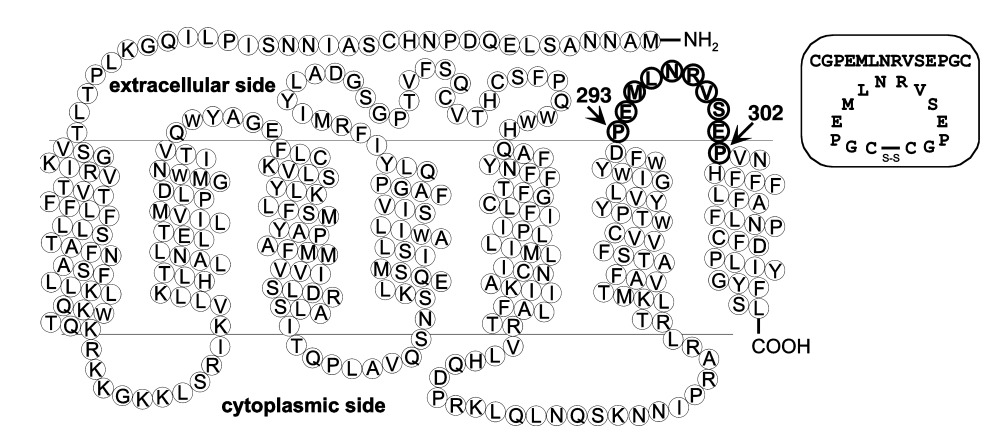


Figure 6. Primary sequence and proposed topology of mouse gonadotropin-releasing hormone (GnRH) receptor. The residues of the third extracellular loop are highlighted in bold typeface. For the synthetic peptides (in the box) a disulfide bridge was introduced between the cysteine residues to mimic the conformational constraints of the loop.

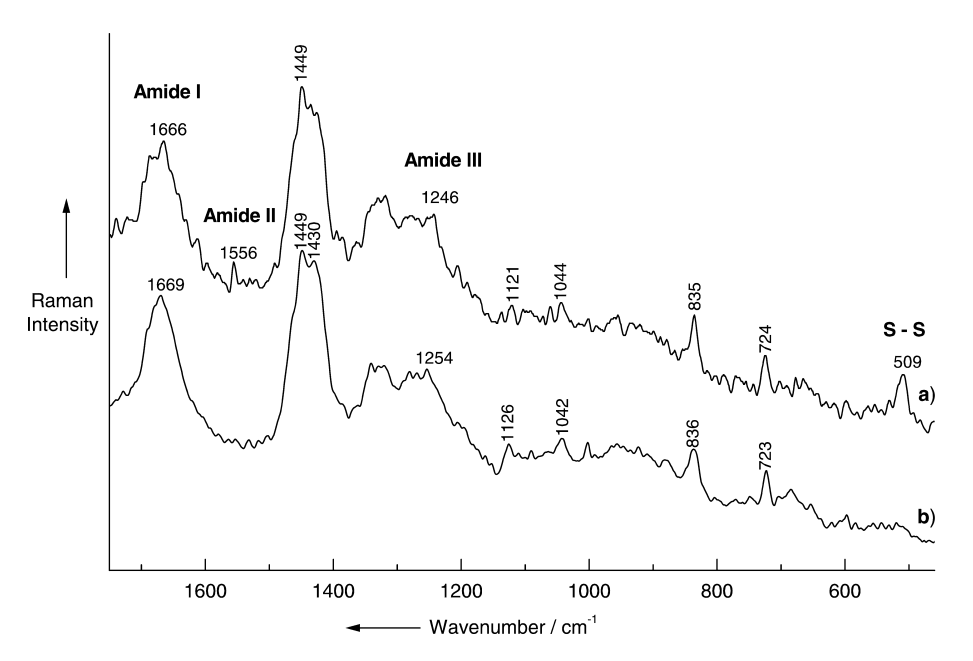


Figure 7. FT-Raman spectra of the third extracellular loop of mouse gonadotropin-releasing hormone receptor, taken from lyophilized peptide sample in a) the cyclic form and b) in the linear form. The sharp 509 cm^{-1} line of the cyclic peptide can be readily assigned to the S–S stretching vibration of the disulfide bridge.

were significantly high at 1666 and 1669 cm $^{-1}$, respectively. This indicated a low degree of hydrogen bonding, which is typical in unordered structure. The amide III band, which originates mainly from C $^-$ N vibrations coupled with N $^-$ H in-plane bending vibrations, appeared at 1248 cm $^{-1}$, supporting the interpretion of a predominantly unordered structure. The CD signals of the ECL3 peptides exhibited a superposition of mainly unordered structure with partial contributions from β -sheet structure. NMR data demonstrated the presence of a β -hairpin among an ensemble of largely disordered structures in the cyclic peptide. Inspection of the NOESY spectrum revealed a medium to strong sequential $\alpha(i)$ – N(i + 1) cross-peaks, which is typical of the pattern expected for an extended or random coil conformation. However, near the central residues of the loop peptide (LNR) the NOE signals provided a first indication that, among the

predominantly random coil-conformational ensemble, there may be a small population of structured species with a local turnlike structure near these residues. Chemical shifts and coupling constants of the linear and cyclic peptides were examined to provide support for this suggestion.

The data obtained from CD and 2D NMR spectroscopy corroborated the Raman results and confirmed that the synthetic ECL3 peptides, both in the cyclic and in the linear forms, are not helical, as has been proposed for the ECL3 receptor domain,[65] but rather have an unordered conformation with some minor contributions from the β -sheet structure. The observations strongly supported the hypothesis that the tendency of the synthetic ECL3 peptides from the GnRH receptor to adopt a loop structure with a β -turn is a reliable indicator of the ability of the loop to assume an active conformation by induction. The study has demonstrated that the application of micro- and FT-Raman spectroscopy as a complement to 2D NMR spectroscopy can provide further insights into the structure function relationship of the extracellular loop of a membrane protein. The acquired structural information has thus contributed to an understanding of to what extent the conformation of the third extracellular loop may play a role in receptor binding and activation.

Raman Spectroscopy on Organically Modified Implants

Restorative medicine and dental surgery addresses increasing interest in the biocompatibility of implant materials, [66] because there is still incomplete knowledge about the interaction mechanisms between biological and inorganic implant material. Applications of Raman and near-IR Raman spectroscopy have been reported in the field of dental health care. The spectroscopic methods were successfully used to distinguish carious lesions from sound hard tooth tissue. [67, 68] The influence of the coating material (hydroxyapatite), which is actively involved in the mineralization of ongrowing bone, was investigated by near-IR FT-Raman spectroscopy on hydroxyapatite-coated implants in dog femurs. [69] The bone growth on implants and the rejection of the implant strongly depends on the physical and chemical

properties of the implant surface. [70-72] It is expected that the application of sol – gel chemistry [73] will improve the biocompatibility of orthopedic and dental implants. The basic principle of the sol – gel method addresses the stimulation of the adhesion of load bearing cells (such as osteoblasts) on the implant surface (Figure 8).

To achieve biocompatibility of the inorganic material, titanium implant surfaces have been chemically modified by the sol–gel technique. Therefore, titanium(IV) ethoxide was connected to L-lysine, L-tyrosine, and L-cysteine following the procedure described by Schubert et al., [74] which results in layers ($\approx 1~\mu m)$ of amino acids on the implant surface. For coating the surface both the dip coating or the spin coating techniques have been applied, resulting in layers with thickness above or below 1 μm , respectively.

Various Raman techniques have been used to obtain information about the structural orientation of amino acids on the surface. [75, 76] Conventional Raman spectra have been recorded with the 647 nm line of a krypton ion laser from both the pure titanium surface and from the chemi-

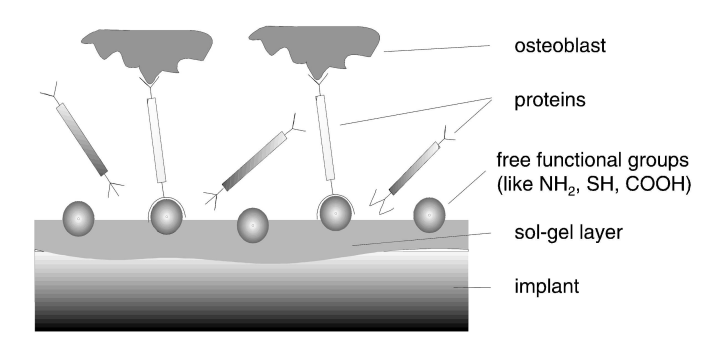


Figure 8. Schematic representation of a chemically modified implant surface in a physiological medium.

cally modified surface. In order to avoid photodegradation all spectra were recorded in a 90° scattering rotating configuration. However, because of the extremely low thickness of the layer no other Raman bands besides the TiO_2 bands have been observed from the organically modified implant surface (Figure 9a).

Therefore, the SERS method has been applied to overcome the problem of low sensitivity. A thin layer (3 nm) of silver was deposited by vapor deposition on top of the substrate. In Figure 9 both spectra, from conventional Raman and SERS spectroscopy, are displayed. The comparison of the SERS and of the normal Raman spectra revealed a considerable enhancement of selective vibrational modes of the sol – gel layer of the modified substrate, leading to a refinement of the structural information (inset of Figure 9 c). The coating consists of bridged surface complexes of TiO₂/Lys with the L-lysine ligand bound to

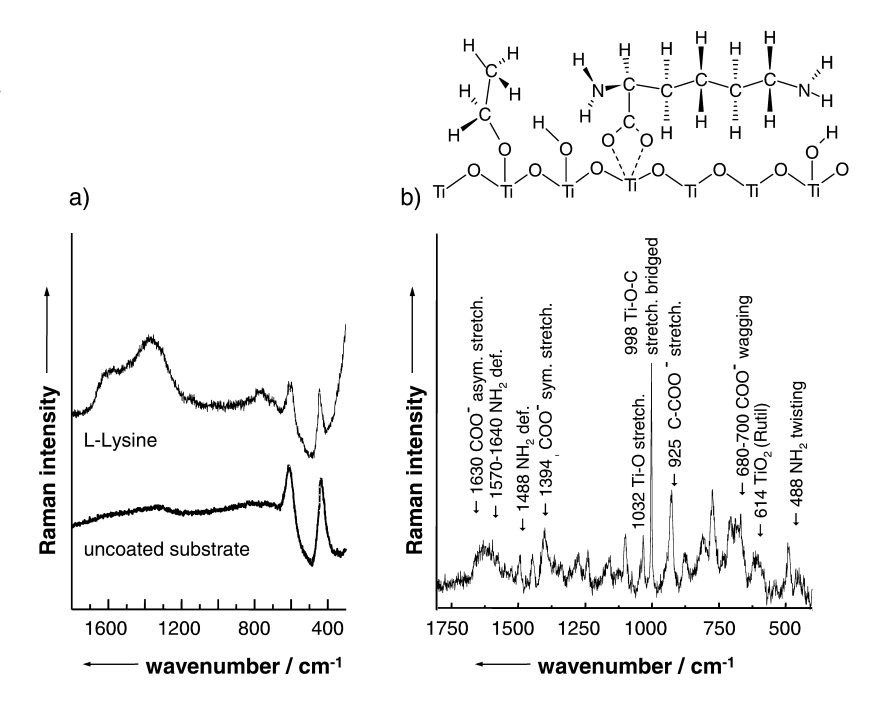


Figure 9. a) Conventional Raman spectrum of the uncoated oxidized titanium substrate and of the titanium substrate modified with L-lysine. b) SERS spectrum of the titanium substrate modified with L-lysine. Inset: Representation of the orientation of L-lysine according to the SERS spectrum.

the titanium dioxide through the carboxylic group (inset in Figure 9). Further coordination through the neighboring ammonium group of the amino acid also appears probable. The enhancement of the C–H stretching vibrations indicates a parallel or possibly tilted orientation of the alkane chain of the molecule relative to the TiO_2/Ag interface. The detection of SERS signals assignable to an amino group implies that the γ -NH $_2$ is not bound to the underlying titanium dioxide but is freely available for further complexation.

The structural characterization of the modified surface layers may potentially contribute to a detailed investigation of the most appropriate modifying ligands. The study revealed that SERS techniques are extremely suited to the investigation of such systems. There is a considerable enhancement of the Raman signals from molecules or functional groups, which are oriented next to the SERS-active metal surface. Furthermore the specific surface selection rules allow for conclusions about the geometry of the surface complexes.

Structural Studies on Soil Components: Humic Acid

The structural characterization of humic acids as well as the determination of their complexation behaviour is of great interest in environmental science. Humic acid occurs in soil and ground-water and is involved in many chemical and biological processes taking place in terrestrial and aquatic environments. The knowledge of the chemical properties is essential for the development of precise ecological models for predictions on the remedy and detoxification of anthropogenic compounds and even of nuclear waste.^[77,78] Yang et al. highlighted the use of Raman, FT-Raman, and SERS techniques for the study of humic substances.^[79]

REVIEWS

A sample of humic acid taken from a British oak forest has been studied by conventional Raman spectroscopy excited with the 647 nm laser line of a Kr⁺ laser. However, the obtained vibrational information from the Raman signals was poor due to strong fluorescence of the sample. The change of the excitation wavelength (1064 nm) slightly improved the spectra, which showed only two broad Raman bands. The investigation of the absorption spectrum of the humic acid in aqueous solution (Figure 10 a) revealed that the sample predominantly absorbs in the visible range of the electromagnetic spectrum. By decreasing

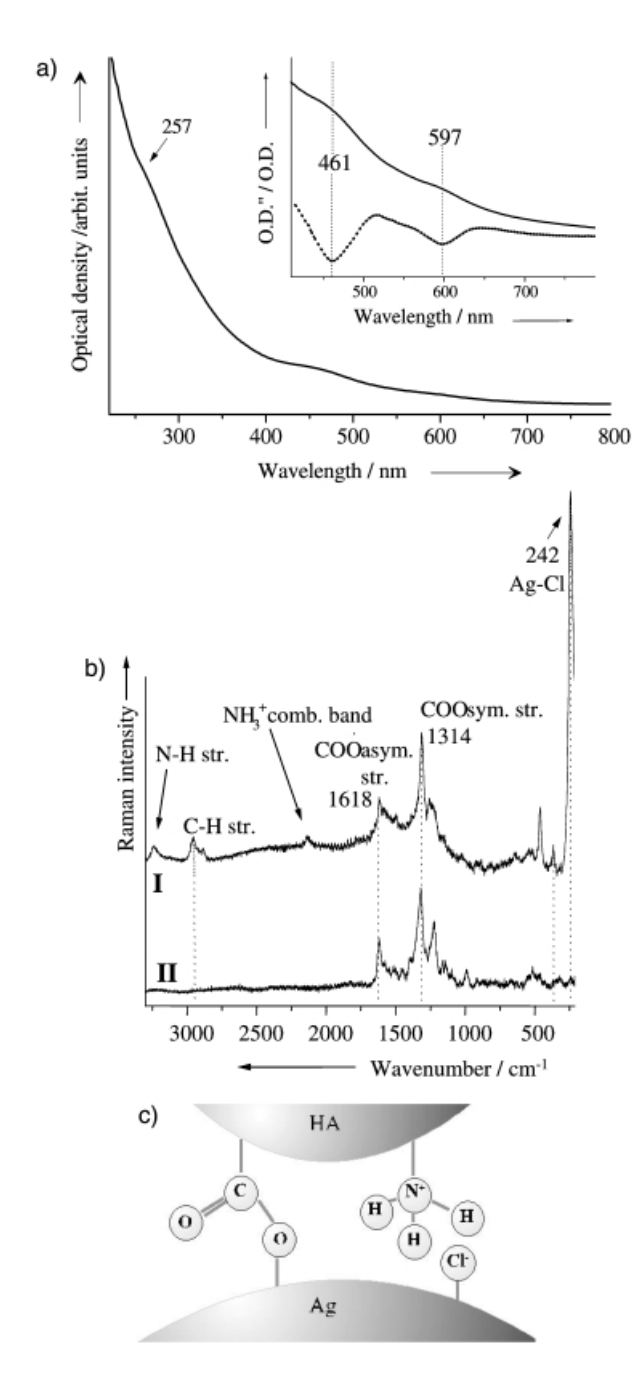


Figure 10. a) Absorption spectrum of the humic acid dissolved in water. Inset: Enhanced part of the spectrum (solid line) and the second derivative (dotted line). b) SERS spectrum of humic acid from an oak forest adsorbed on a roughened silver electrode (I) and on a silver island film (II). c) Proposed adsorption geometry.

the wavelength for excitation the optical density was increased. Three band shoulders (at 257, 461, and 597 nm) were detected in the spectrum (inset in Figure 10 a). These absorption features can be interrelated with electronic transitions involving a large system of conjugated aromatic, allylic, or hetero π -bonds building the molecular skeleton.

In order to enhance the signal SERS, experiments were performed where electrochemically roughened silver electrodes in an electrochemical cell containing 0.1 $\rm M$ KCl solution as electrolyte and thermally evaporated silver films (thickness 15 nm) have been used as substrates. The presence of the metal results in a quenching of the fluorescence (Figure 10 b). The most prominent band observed in the SERS spectrum of the roughened electrode ($\lambda = 647$ nm, Figure 10 b, spectrum I) appears at 242 cm $^{-1}$. This line can be readily assigned to the Ag $^{-1}$ Cl stretching of adsorbed terminal chloride anions.

The vibrational assignment of the recorded Raman bands and of other spectral features in the "fingerprint" region is not unambiguous. The main difficulty arises from the still incompletely determined molecular structure of humic acids. The intensity pattern between 1300 and 1600 cm⁻¹ is characteristic for symmetric (ν_s) and antisymmetric (ν_{as}) stretching vibrations of the COO- group (Figure 10b). Comparing these results with the vibrational modes of the free carboxylates, ν_s exhibits a considerable downshift while $\nu_{\rm as}$ is upshifted. The spectral features are thus similar to the observed peaks of unidentate metal - acetate complexes, that were reported earlier by Nakamoto. [80] The binding mechanism of the carboxylic group results in an enhancement of the double bond character of one of the C-O bonds. The other C-O bond is directly coordinated to the silver and mainly shows the characteristics of a single bond (Figure 10c).

With the information obtained from the SERS spectra it appears most likely that one of the carboxylic groups is involved in the adsorption of the humic acid on the silver surface. The presence of coadsorbed Cl⁻ ions causes an additional coordination through a terminal ammonium group (see Figure 10c). Thus, the SERS studies provided information on the mechanisms of binding and/or complexation configurations of humic acids. All 282, 811

Spectroscopy of Plant Tissue and Micro-Organisms

Alkaloid Studies by FT-Raman Spectroscopy

Naphthylisochinoline alkaloids are derived as secondary metabolites from tropical liana of the family *Ancistrocladaceae*, which form a new class of natural products. Some of the alkaloids are promising with respect to their fungicidal and antimalarial activity. Fluorescence microscopic studies and in vivo NMR imaging have been applied prior to Raman studies reported by Urlaub et al. (see ref. [84] and references therein). FT-Raman spectra were acquired with a microscope attached to a FT-spectrometer using the 1064 nm line of a cw Nd:YAG laser for excitation. Even though the chemical structures of the various alkaloids (ancistrocladine, ancistrocladisine, ancistrocladidine, ancistrocladinine, and ancistroheynine A) are very similar, the

distinct lines in the Raman spectra allowed a differentiation between each of the alkaloid species.

The systematic spectroscopic study of different parts of the plant resulted in the spectroscopic localization of different alkaloids in various parts of the plant. Figure 11 a displays a

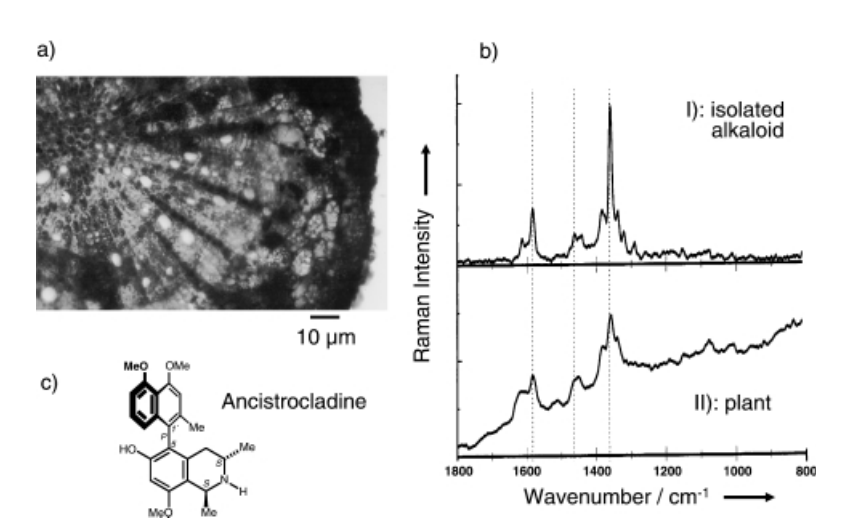


Figure 11. a) Fluorescence image of the root cross-section ($\lambda_{\rm ex} = 365$ nm; image H. Schneider, U. Zimmermann, University of Würzburg). b) FT-Raman spectra of I) a single white fluorescing inclusion and II) of ancistrocladine. c) Molecular structure of ancistrocladine.

microscopic cross-section of the root of *A. heyneanus*, revealing spherical crystalline inclusions (\approx 5 µm) with a weak fluorescence upon irradiation at 365 nm. The characterization of these crystals in the plant cells was achieved by micro-Raman spectroscopic studies. Although some fluorescence is still observed in the in situ spectrum of the root at 1064 nm (Figure 11 b), characteristic Raman peaks can be clearly observed on top of the background. From spectra I and II of Figure 11 b, the observed Raman bands could be ascribed to the alkaloid ancistrocladine (Figure 11 c).

Raman spectra with a good signal-to-noise ratio can be obtained possibly due to the crystalline form of this alkaloid in the cells. Since the laser spot can be focused on a single crystal, the data of the alkaloid can be taken exclusively.

The study demonstrated the application of micro-FT-Raman spectroscopy with good spatial resolution ($\approx 5~\mu m)$ to investigate the distribution of different alkaloids in particular parts of the plant. SERS studies also have been performed. However, after penetrating the plant cross-section with silver colloid no Raman signal could be obtained.

Taxonomic Analysis on Oil-Proliferating Plants

The *Laminaceae* plants and their extracted essential oils are well known for numerous therapeutic effects and wide medical applications. Many common plants such as thyme, oregano, and mints are members of this family.

In order to investigate in vivo the chemical composition of these herbs, several biological and spectroscopic obstacles must be ruled out. First of all, biological raw materials show qualitative and quantitative differences in their chemical composition, which originate from annual growing variations, different soils,

solar radiation, rain, and fertilization. Furthermore, each species consists of various subspecies or hybrids with a specific chemical composition.

Mint plants of the genus *Mentha* exhibit a high capability of hybridization and thus the taxonomic differentiation is complex. The main components of mint oils are monoterpenes, such as menthol, menthone, and carvone, which appear in varying concentrations in the different species. The characteristic scent of each taxon is caused by other monoterpenes (including cineole and limonene) that are present only at low concentrations. Rapid characterization and precise classification should therefore be possible using the information from Raman spectroscopy to distinguish different mint species via the monoterpenes of their essential oils.

The classical analysis is using a combination of extraction methods and GC or HPLC, which possibly cause modifications in the chemical nature of the compounds. In order to avoid these complications, Raman spectroscopy is applied as a non-destructive tool for the investigation of mints. It

has been shown before that microstructure samples (such as plant cross-sections) can be investigated by a micro-Raman setup. The use of a micro-Raman setup in combination with the silver colloid enables us to investigate the essential oils of *Mentha* in the glandular trichomes itself. In Figure 12 a a picture of the plant $Mentha \times piperita$ is shown. The enlargement represents a micrograph of a glandular trichome, which provides the storage of the essential oil. When such a plant cell is investigated under the microscope and is excited by the

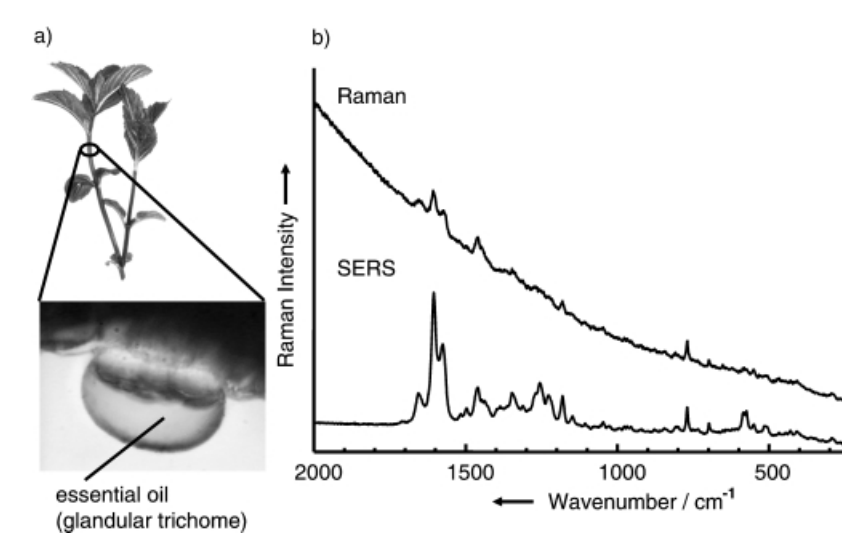


Figure 12. a) Image of Mentha × piperita. The enlargement shows a micrograph of a glandular trichome, where the essential oil is stored. b) Raman and SERS spectra taken from such an oil cell. The applied Raman excitation was 514 nm for both spectra.

514 nm line of an Ar⁺ laser the spectrum is dominated by fluorescence. The spectrum of the essential oil appears quite weak and is masked by strong fluorescence. The fluorescence is reduced considerably when silver colloid is added, (Figure 12b). Since the colloids are not able to penetrate through the cuticular wax, a SERS enhancement can be obtained only from molecules of the essential oil, which can penetrate into the cuticular wax. Otherwise the colloids just quench the fluorescence, which might be caused by impurities from the outer plant regions. However, the SERS spectra reveal mainly vibrations of various monoterpenes with few signals belonging to the cell background.

For the taxonomic assignment two species of mints—the hybrid $Mentha \times piperita$ and $Mentha \, spicata$ —have been investigated. [86, 82, 87] The main components of $Mentha \times piperita$ are menthol and menthone, whereas the main component of $Mentha \, spicata$ is the monoterpene carvone. The SERS spectra show sufficient differences, most apparent in the region of 1550 to 1700 cm⁻¹ to distinguish between both species (see Figure 13). Although the SERS spectra from five taxa of $Mentha \times piperita$ and from two taxa of $Mentha \, spicata$ indicate a high degree of similarity, several spectral features still allow one to distinguish between the various taxa (Figure 13).

As we are interested in the characterization of the taxa below the species, such as subspecies or varieties, we have applied a hierarchical cluster analysis as a complement to SERS spectroscopy. For an overview of applying statistical and mathematical

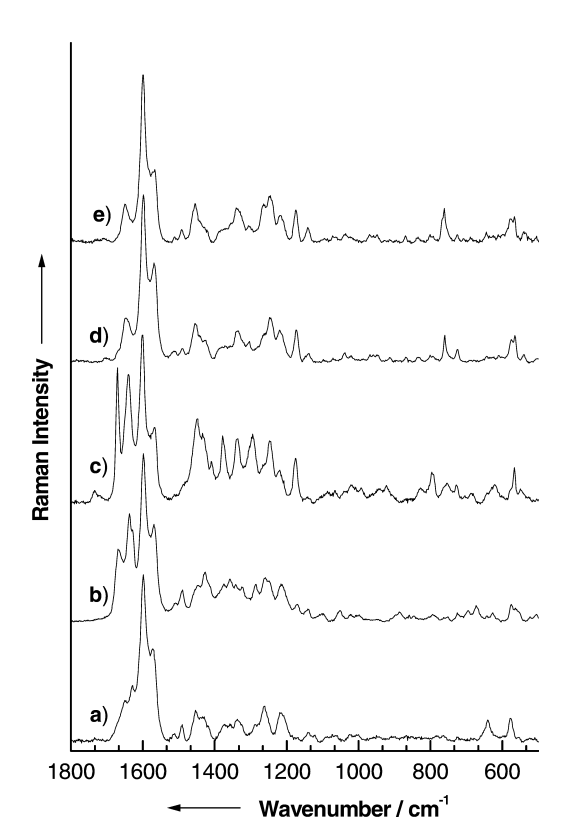


Figure 13. Raman spectra of mints a) M. spicata L. ssp. spicata, b) M. spicata L. ssp. crispata, c) M. \times piperita L. nm. citrata, d) M. \times piperita L. var. pallescens pallescens, and e) M. \times piperita L. var. piperita f. piperita (black mint).

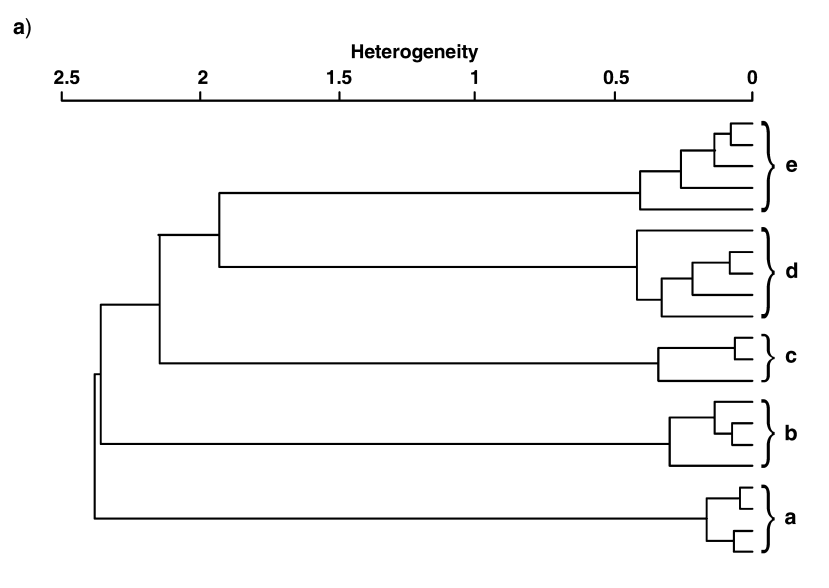
methods for analyzing chemical data (chemometrics) see ref. [88]. In order to minimize the effect of alternating compositions in the essential oils (due to annual variation) we have used the signals of the cuticular wax to extract the characteristic information. The Raman spectra of the different mints are reproducible for a certain collection date, but in some cases differ drastically during the year because of the changing composition during the season. This effect must be taken into account when a hierarchical cluster analysis is performed. Figure 14a shows 21 spectra of the five different mints from a certain date that are used for the calculation. The spectra were pretreated by a baseline correction followed by the second derivative. In order to select the appropriate spectral range, several parts of the spectra were evaluated, for example, the Raman signals of the cuticula that appeared between 1620 and 1160 cm⁻¹ or the Raman bands of the essential oils from the two ranges within $1690 - 1620 \text{ cm}^{-1}$ and $1120 - 500 \text{ cm}^{-1}$. The best results were achieved by performing the hierarchical cluster analysis in the spectral range between 520 and 1690 cm⁻¹. The spectral distance is calculated with the factor algorithm (factor 5) using a vector normalization. This method allows us to present the spectra as a linear combination of factor spectra, Equation (1), where vector \boldsymbol{a} represents spectrum a, f_i is the factor spectra, and T_{ia} are the score coefficients.^[89] The score coefficients T_{ia} are used for the calculation of the spectral distance D_r Equation (2).

$$a = T_{1a} \cdot f_1 + T_{2a} \cdot f_2 + T_{3a} \cdot f_3 + \cdots$$
 (1)

$$D = \sqrt{\sum_{i} (T_{ia} - T_{ib})^{2}}$$
 (2)

Using Ward's algorithm for cluster analysis, we see that the two species M. spicata (a) and Mentha × piperita (e) are well separated. The taxa below the species can also be distinguished. Figure 14b) shows a dendrogram of a classification based on 38 spectra of the five different mints measured at four time points during the growing season. As the composition of the essential oils changes, a more elongated pretreatment of the spectra is required. This time the spectra are smoothed after the baseline correction followed by a minimum - maximum normalization. The cluster analysis is performed in the file limits (500 -2000 cm⁻¹). The spectral distance is calculated with the factor algorithm using a factor of ten and applying vector normalization. When using Ward's algorithm for the cluster analysis, a discrimination of the two species can be visualized. It is also possible to distinguish between the subspecies and varieties because the spectra of the single taxa are more divergent than the spectra measured at one collection time.

The investigations have demonstrated that the method allows one to monitor subtle differences in the essential oil contents of the mints due to seasonal variation, thus providing valuable information for the producers of fragrances and aromatherapy products. Raman spectroscopy may serve to develop a routine measurement technique for the quality control of the essential oils in plants. It may be used as a complementary or alternative method to IR or NIR spectroscopy which has been used so far for quality control of essential oils.^[37, 90, 91]



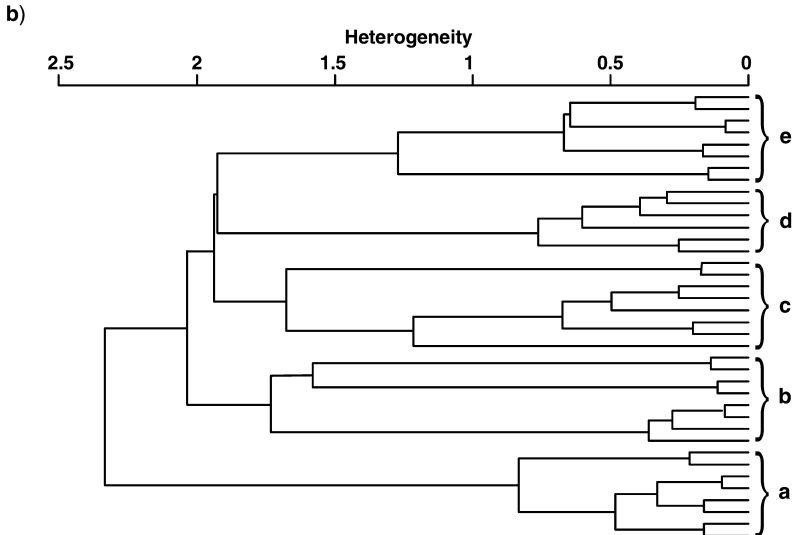


Figure 14. The heterogeneity of the Raman spectra of different mints calculated with a) the spectra of one collection time and b) the spectra taken during a growing season. The letters a-e correspond to the different mint taxa of Figure 13.

Localizing and Identifying Single Bacteria

Medical and biological science is challenged by the nonambiguous identification of micro-organisms such as bacteria and viruses. Nonpathogenic and pathogenic contaminations are critical factors in numerous industrial processes (for example clean-room production of cosmetics and drugs in the food and pharmaceutical industry). The most common identification methods use morphological evaluation in combination with specific tests for the micro-organism's ability to grow in various media. However, the identification of micro-organisms usually becomes a lengthy process when time-consuming cultivation is required (up to 72 hrs). An overview on the various approaches discussed in literature is reviewed by lvnitski et al.^[92]

What are the requirements for fast taxonomic assignments of micro-organisms? First, a single cell or only a small number of

micro-organisms should be necessary for an unambiguous analysis. Second, the identification should be performed on a small time-scale (within a few seconds, up to minutes), and, third, the assignment needs to be highly specific. Vibrational spectroscopic techniques such as Raman^[93-95] and IR^[96-102] spectroscopy in combination with chemometric techniques or neural networks[103, 104] allow a direct and fast identification of micro-organisms. Cell suspension and dried films of micro-organisms have been investigated by FT-Raman $^{\left[105,\ 106\right]}$ as well as by UV-RR spectroscopy. $^{\left[107\right]}$ Nelson and Sperry have studied bacterial suspensions, bacterial colonies, and bacterial tribes consisting of 1 to 50 cells, and identified the different species from the UV-RR spectra.[108] The group of Puppels has been able to perform the microbial identification by applying confocal NIR-Raman spectroscopy[109-111] on a sample volume in the range of 1 μm³. Single cells have been investigated and identified on CaF₂ plates by Schuster et al.[112]

Gessner et al. have performed the taxonomic investigation of single bacteria.[113] In the first step they concentrated on micro-organisms which contain a chromophore (β -carotene, sarcinaxantin) in the cytoplasma membrane. Therefore, different types of bacteria were cultivated, mixed, and a smear of the mixture was then investigated on a glass plate. By using a confocal micro-Raman setup, single microorganisms have been investigated. The laser focus was approximately 1 µm (514 nm). An image of such a mixture of Rhodotorula rubra and Micrococcus luteus on a glass plate is displayed in Figure 15a. The different morphology readily allows us to distinguish between both types of bacteria. However, comparing the two carotenoids, which are β -carotene in *Rhodotorola rubra* and sarcinaxantin in Micrococcus luteus the task was to distinguish both bacteria using the molecular vibrations of the chromophore. Figure 15 b shows four different Raman spectra taken at the four positions on the sample. Spectrum A in Figure 15 b originates from the glass plate, whereas spectra B and D reveal the

characteristic Raman information of the two chromophores. It can be recognized that although the molecules are similar the Raman band near 1500 cm⁻¹, which corresponds to the C=C vibration, appears with a moderate Raman shift for both species. Spectrum C was taken when the laser was positioned on the mixture of both bacteria. By scanning over the displayed area the obtained Raman information allows one to localize and identify the two bacteria. It is important to note that because of the RR effect of the chromophors at 514 nm excitation no other molecules should contribute to the Raman spectrum.

Raman Spectroscopy Investigation of Biological Materials by use of Etched and Silver-Coated Glass Fiber Tips

As has been shown so far, Raman spectroscopy is well suited for identifying compounds of biological material, but when working

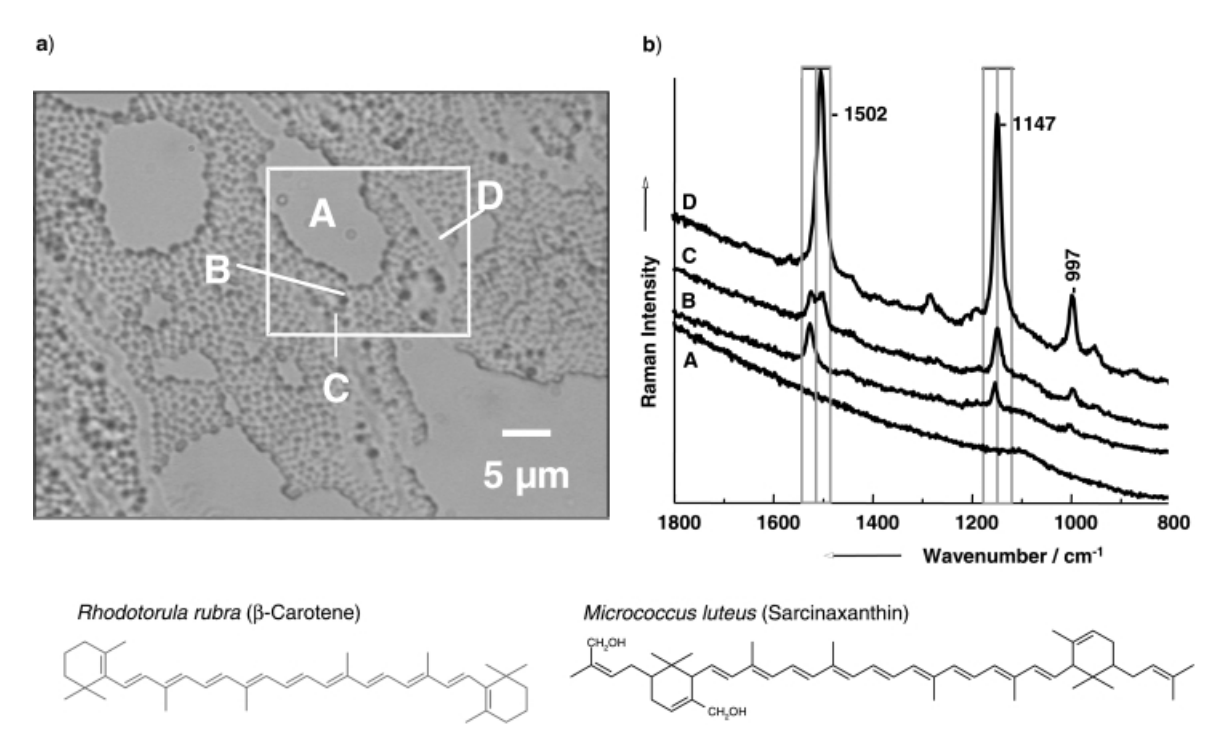


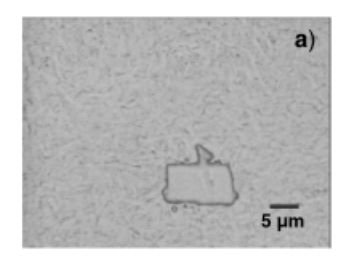
Figure 15. Localization and identification of Rhodotorola rubra and Micrococcus luteus of a bacteria smear prepared on a glass plate. a) The spatial distribution of the cell on the glass plate and b) the corresponding Raman spectra that were recorded from four selected positions (labeled A – D). The molecular structures for both molecules are displayed. For more information see text.

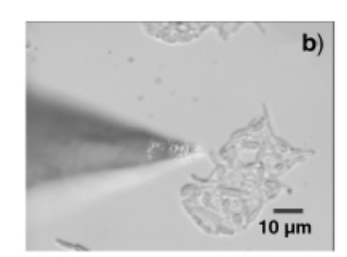
with biological samples, several problems may arise: a) the very small substance quantities are often below the detection limit of Raman spectroscopy, b) a lot of biological samples show fluorescence that is orders of magnitude more intense than the Raman signal, and c) biological samples are very sensitive and might be destroyed by the Raman excitation laser. One method to overcome these problems is the SERS technique, as has been pointed out in the previous sections. However, the high amounts of heavy metals (such as silver, gold, or copper) required for the SERS technique often leads to the destruction of the highly sensitive biological samples. In order to reduce the metal concentration Gessner et al. used silver-coated glass fiber tips with diameters in the submicron size range as the SERS substrate. An additional major advantage of using these glass fiber tips is the possibility of exact positioning of the tip and therefore the exciting laser to the designated area of the biological sample to be investigated. The fiber tips are prepared by the tube etching method of Stöckle et al.[114] For the etching process the glass fiber ends are immersed for 2 h in hydrofluoric acid, which is covered with p-xylene to reduce evaporation of the HF. The whole experiment is set on a muting pad to reduce vibrations during the etching process. After the etching the plastic jacket is removed from the fiber by dissolving in hot concentrated sulfuric acid. The etched glass fiber tips are silver coated by thermal evaporation in a modified sputter coater (Edwards S150B).

Due to the small dimensions of the fiber and the fact that the main light intensity is emanating from the fiber tip, the spatial resolution of this method is very good. This was verified by an experiment with crystal violet solution as a model substance where a spatial resolution of 200 – 500 nm, depending on the tip that was used, could be reached.

An impressive example for the practicability of this method is the investigation of monolayers of the yeast Rhodotorula mucilaginosa (rubra) on a glass slide. The main problem with laser spectroscopy on micro-organisms is their sensitivity toward photoinduced destruction. Figure 16 a shows the attempt of an area scan with a conventional micro-Raman setup on a smear of the yeast R. mucilaginosa on a glass slide. It can be seen that the area scanned by the laser is practically cleansed of all yeast cells and no spectrum could be obtained by this method. A micro-Raman spectrum was therefore recorded directly from the agar plate on which the yeast was grown. The multilayered cell colonies could withstand the laser long enough to provide spectrum 2 of Figure 16 c. Figure 16 b shows a glass fiber tip at a small yeast cell colony on a glass slide. With the fiber setup shown [Figure 16b] it was possible to obtain spectrum 3 in Figure 16c without destroying the yeast cells during the measurement. Therefore, it should be possible to measure micro-organisms directly from contaminated surfaces without growing pure strains. Spectrum 1 in Figure 16c shows a bulk spectrum of β -carotene in ethanol as a reference. The slight shift that is observable between the ethanolic β -carotene spectrum and the spectrum of R. mucilaginosa is due to the different environments in which the spectra are recorded.[115] It is possible to obtain spectra from the micro-organisms with fiber tips due to the considerably reduced laser power.

This work illustrates that it is possible to reduce the laser power used for Raman measurements of biological samples by two orders of magnitude. Further, it is possible to illuminate only





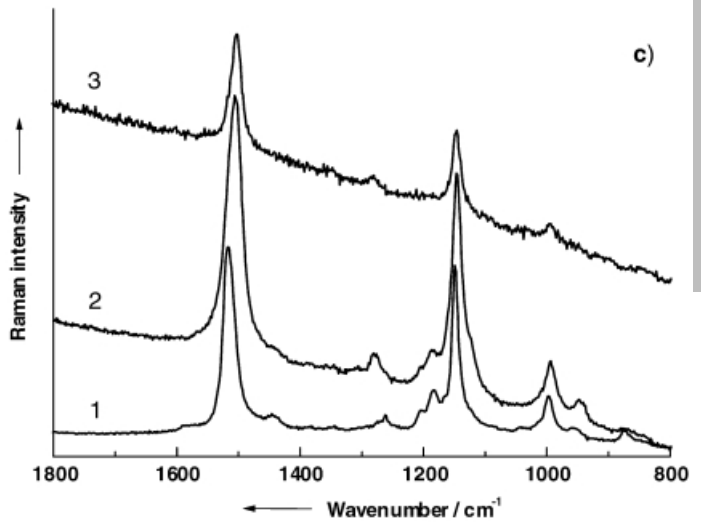


Figure 16. a) Microphotograph of a smear of the yeast Rhodotorula mucilaginosa on a glass slide. The erased area was destroyed by the laser. b) Illuminated SERS fiber tip in close proximity of a small yeast colony. c) The Raman spectra taken from β -carotene and of the yeast R. mucilaginosa under differing experimental conditions: 1) β -carotene in ethanol, 10 mm sample cell, micro-Raman setup, 60 mW laser power; 2) R. mucilaginosa on agar, micro-Raman setup, 60 mW laser power; and 3) a small yeast colony of R. mucilaginosa prepared on a glass slide, SERS fiber tip, 0.2 mW laser power.

the target area of the sample by using etched and silver coated glass fiber tips as the SERS probe. This considerably reduces the photoinduced stress generated by the excitation laser and therefore increases the time the sample can withstand photodestruction. The reduced photodestruction results in the requirement of smaller sample amounts. Especially for microorganisms, it would reduce the growth periods considerably or would make it completely redundant because less cells are necessary for a spectroscopic identification. The good spatial resolution of the fiber tip (< 1 μ m) is another advantage because it enables the determination of the spatial distribution of certain substances in a sample; also, a very small substance amount can be measured on a heterogeneous sample.

Summary

In the last decades powerful Raman methods have been developed by several research groups, which offer sophisticated tools well-suited for particular needs in biospectroscopy. Typical problems often encountered in Raman biospectroscopy consist of the intrinsically low scattering cross-section and the occurrence of fluorescence. In the present Review we have demonstrated by a range of applications that modern techniques in

Raman spectroscopy provide means to circumvent these draw-backs, for example by the application of signal enhancing and fluorescence quenching techniques. Furthermore, we pointed out that each biological system requires careful selection of the most appropriate experimental setup, of the adequate excitation source and particular sample preparation in order to obtain structural information from biological molecules.

J.P. gratefully acknowledges the financial support of the Deutsche Forschungsgemeinschaft and the Fond der Chemischen Industrie. He was also supported by the award of the Bayerisches Habilitationsstipendium. The authors are most grateful to Prof. Dr. W. Kiefer for the technical and the financial support, for helpful scientific discussion as well as the use of the Raman laboratories. The funding of the research project FKZ 13N7511 within the framework "Laser-Biodynamik" from the BMBF in Germany is gratefully acknowledged.

- [1] G. J. Puppels, T. C. Bakker, P. J. Caspers, R. Wolthuis, M. van Aken, A. van der Laarse, H. A. Bruining, H. P. J. Buschmann, M. G. Shim, B. C. Wilson in *Handbook of Raman Spectroscopy; Practical Spectroscopy, Vol.* 28 (Ed.: I. R. Lewis), Dekker, New York, NY, 2001, pp. 540 574.
- [2] L.-P. Choo-Smith, H. G. M. Edwards, H. P. Endtz, J. M. Kros, F. Heule, H. Barr, J. S. Robinson, Jr., H. A. Bruining, G. J. Puppels, *Biopolymers* 2002, 67, 1 – 9.
- [3] P. Carey, Opt. Pura Apl. 1984, 17, 219 226.
- [4] S. A. Asher, Anal. Chem. **1993**, 65, 59A 66A.
- [5] S. A. Asher, Anal. Chem. 1993, 65, 201A 210A.
- [6] S. A. Asher, Annu. Rev. Phys. Chem. 1988, 39, 537 588.
- [7] C. M. Jones, T. A. Naim, M. Ludwig, J. Murtaugh, L. Perry, J. M. Dudik, C. R. Johnson, S. A. Asher, TrAC Trends Anal. Chem. 1981, 4, 75 50.
- [8] S. A. Asher, Methods Enzymol. 1981, 76, 371 413.
- [9] J. C. Austin, T. Jordan, T. G. Spiro, Adv. Spectrosc. 1993, 20, 55 127.
- [10] E. A. Carter, H. G. M. Edwards in *Practical Spectroscopy, Vol. 24* (Ed.: H.-U. Gremlich), Dekker, New York, NY, 2001, pp. 421 475.
- [11] G. J. Thomas, Jr., Annu. Rev. Biophys. Biomol. Struct. 1999, 28, 1 27.
- [12] G. J. Puppels, C. Otto, J. Greve, *Trends Anal. Chem.* **1991**, *10*, 249–253.
- [13] G. J. Puppels, M. V. Rooijen, C. Otto, J. Greve in *Fluorescent and Luminescent Probes for Biological Activity, Vol. 1* (Ed.: W. T. Mason), Academic, London, 1993, pp. 237 258.
- [14] R. Salzer, G. Steiner, H. H. Mantsch, J. Mansfield, E. N. Lewis, Fresenius' J. Anal. Chem. 2000, 366, 712 – 716.
- [15] K. Kneipp, H. Kneipp, I. Itzkan, R. R. Dasari, M. S. Feld, Chem. Rev. 1999, 99, 2957 – 2975.
- [16] K. Kneipp, H. Kneipp, I. Itzkan, R. R. Dasari, M. S. Feld, Springer Ser. Chem. Phys. 2001, 67, 144–160.
- [17] K. Kneipp, H. Kneipp, I. Itzkan, R. R. Dasari, M. S. Feld, J. Phys.: Condens. Matter 2002, 14, R597 – R624.
- [18] E. B. Hanlon, R. Manoharan, T.-W. Koo, K. E. Shafer, J. T. Motz, M. Fitzmaurice, J. R. Kramer, I. Itzkan, R. R. Dasari, M. S. Feld, *Phys. Med. Biol.* 2000, 45, R1 R59.
- [19] L. A. Nafie, G.-S. Yu, T. B. Freedman, Vib. Spectrosc. 1995, 8, 231 239.
- [20] L. A. Nafie, D. Che, Adv. Chem. Phys. 1993, 85, 105 149.
- [21] L. A. Nafie, T. B. Freedman, *Methods Enzymol.* **1993**, *226*, 470 482.
- [22] L. D. Barron, L. Hecht in Circular Dichroism, Vol. 2 (Eds.: N. Berova, K. Nakanishi, R. W. Woody), Wiley-VCH, New York, NY, 2000, pp. 667 701.
- [23] G. Puppels, J. Raman Spectrosc. **2002**, 33, 496 592.
- [24] Handbook of Vibrational Spectroscopy, Vol. 5 (Eds.: J. M. Chalmers, P. R. Griffiths), Wiley, Chichester, 2002.
- [25] B. Schrader, Infrared and Raman Spectroscopy—Methods and Applications, VCH, Weinheim, 1995.
- [26] W. Kiefer, H. J. Bernstein, J. Mol. Struct. 1972, 43, 366 381.
- [27] W. Kiefer in Infrared and Raman Spectroscopy—Methods and Applications, Vol. 21 (Ed.: B. Schrader), VCH, Weinheim, 1995, pp. 465 – 517.

Raman Spectroscopy in the Life Sciences

REVIEWS

- [28] M. Fleischmann, P. J. Hendra, A. J. McQuillan, *Chem. Phys. Lett.* **1974**, *26*, 163 166
- [29] J. A. Creighton in Spectroscopy of Surfaces, Vol. 21 (Eds.: R. J. H. Clark, R. E. Hester), John Wiley & Sons, New York, NY, 1988.
- [30] D. A. Weitz, M. Moskovits, J. A. Creighton in Surface-Enhanced Raman Spectroscopy with Emphasis on Liquid – Solid Interfaces, Vol. 2 (Eds.: R. B. Hall, A. B. Ellis), VCH, Deerfield Beach, FL, 1986, pp. 197 – 243.
- [31] M. Moskovits, NATO ASI Ser., Ser. C 1992, 378, 1–15.
- [32] T. Vo-Dinh, Trends Anal. Chem. 1998, 8 and 9, 557 582.
- [33] K. Kneipp, Y. Wang, H. Kneipp, I. Itzkan, R. R. Dasari, M. S. Feld, *Phys. Rev. Lett.* 1996, 76, 2444 2447.
- [34] K. Kneipp, Y. Wang, H. Kneipp, I. Itzkan, R. R. Dasari, M. S. Feld, *Phys. Rev. Lett.* 1997, 78, 1667 1670.
- [35] S. Nie, S. R. Emory, Science 1997, 275, 1102 1106.
- [36] G. C. Schatz, R. P. van Duyne, W. E. Smith, C. Rodger in *Handbook of Vibrational Spectroscopy, Vol. 1* (Eds.: J. M. Chalmers, P. R. Griffiths), John Wiley & Sons, New York, NY, 2002, pp. 759 785.
- [37] B. Schrader, H. Schulz, G. N. Andreev, H. H. Klump, J. Sawatzki, *Talanta* 2000, 53, 35–45.
- [38] T. Hirschfeld, B. Chase, Appl. Spectrosc. 1986, 40, 133 137.
- [39] B. Chase, Anal. Chem. 1987, 59, 881 889.
- [40] C. G. Zimba, V. M. Hallmark, J. D. Swalen, J. F. Rabolt, Appl. Spectrosc. 1987, 41, 721 – 726.
- [41] N. Zimmerer, W. Kiefer, Appl. Spectrosc. 1974, 28, 279 281.
- [42] W. Kiefer, W. J. Schmid, J. A. Topp, *Appl. Spectrosc.* **1975**, *29*, 434–436.
- [43] W. Kiefer in Advances in Infrared and Raman Spectroscopy, Vol. 3 (Eds.: R. J. H. Clark, R. E. Hester), Heyden, London, 1977, pp. 1 42.
- [44] M. Bridoux, M. Delhaye in *Advances in Nonlinear Spectroscopy, Vol. 2* (Eds.: R. J. H. Clark, R. E. Hester), Wiley, Chichester, **1976**, pp. 140 152.
- [45] P. Dhamelincourt in *Handbook of Vibrational Spectroscopy, Vol. 2* (Eds.: J. M. Chalmers, P. R. Griffiths), John Wiley & Sons, New York, NY, 2002, pp. 1419 – 1428.
- [46] W. Kiefer, H. J. Bernstein, Appl. Spectrosc. 1971, 500 501, 609 613.
- [47] M. Lankers, D. Göttges, A. Materny, K. Schasschek, W. Kiefer, Appl. Spectrosc. 1992, 46, 1331 – 1334.
- [48] P. J. Treado, M. P. Nelson in *Handbook of Vibrational Spectroscopy, Vol. 2* (Eds.: J. M. Chalmers, P. R. Griffiths), John Wiley & Sons, New York, NY, 2002. pp. 1429 – 1459.
- [49] M. Bowden, G. D. Dickson, D. J. Gardiner, D. J. Wood, Appl. Spectrosc. 1990, 44, 1679 – 1684.
- [50] D. J. Gardiner, M. Bowden, P. R. Graves, *Philos. Trans. R. Soc. London, Ser. A* 1986, 320, 295 – 306.
- [51] R. Tabaksblat, R. J. Meier, B. J. Kip, *Appl. Spectrosc.* **1992**, *46*, 60 68.
- [52] G. J. Puppels, W. Colier, J. H. F. Olminkhof, C. Otto, F. F. H. de Mul, J. Greve, J. Raman Spectrosc. 1991, 22, 217 – 225.
- [53] G. Rosasco in Advances in IR and Raman Spectroscopy, Vol. 7 (Eds.: R. J. H. Clark, R. E. Hester), Heyden, London, 1980, pp. 223 – 283.
- [54] K. P. J. Williams, G. D. Pitt, D. N. Batchelder, B. J. Kip, Appl. Spectrosc. 1994, 48, 232 – 235.
- [55] L. Baia, K. Gigant, U. Posset, R. Petry, G. Schottner, W. Kiefer, J. Popp, Vib. Spectrosc. 2002, 29, 245 – 249.
- [56] L. Baia, K. Gigant, U. Posset, G. Schottner, W. Kiefer, J. Popp, Appl. Spectrosc. 2002, 56, 536 – 540.
- [57] R. Petry, D. Craik, G. Haaima, B. Fromme, H. Klump, W. Kiefer, D. Palm, R. Millar, J. Med. Chem. 2002, 45, 1026 1034.
- [58] S. C. Sealfon, H. Weinstein, R. P. Millar, *Endocr. Rev.* **1997**, *18*, 180 205.
- [59] E. Pebay-Peyroula, G. Rummel, J. P. Rosenbusch, E. M. Landau, *Science* 1997, 277, 1676 – 1682.
- [60] K. Palczewski, T. Kumasaka, T. Hori, C. A. Behnke, H. Motoshima, B. A. Fox, I. Le Trong, D. C. Teller, T. Okada, R. E. Stenkamp, M. Yamamoto, M. Miyano, Science 2000, 289, 739 – 745.
- [61] P. L. Yeagle, A. Salloum, A. Chopra, N. Bhawsar, L. Ali, G. Kuzmanovski, J. L. Alderfer, A. D. Albert, J. Pept. Res. 2000, 55, 455 465.
- [62] P. L. Yeagle, J. L. Alderfer, A. D. Albert, *Biochemistry* **1997**, *36*, 9649 9654.
- [63] G. Fink in The Physiology of Reproduction (Eds.: E. Knobil, J. Neill), Raven Press, New York, NY, 1988, pp. 1349 – 1377.
- [64] B. J. Fromme, A. Katz, R. W. Roeske, R. P. Millar, C. A. Flanagan, Mol. Pharmacol. 2001, 60, 1280 – 1287.
- [65] R. Sankararamakrishnan, K. Konvicka, E. L. Mehler, H. Weinstein, Int. J. Quantum Chem. 2000, 77, 174 – 186.
- [66] P. Tengvall, I. Lundstrøm, Clin. Mater. 1992, 9, 115 134.

- [67] W. Hill, V. Petrou, Appl. Spectrosc. 1997, 51, 1265 1268.
- [68] W. Hill, V. Petrou, Appl. Spectrosc. 2000, 54, 795 799.
- [69] S. Döpner, F. Müller, P. Hildebrandt, R. T. Müller, Biomaterials 2002, 23, 1337 – 1345.
- [70] S. Kothari, P. V. Hatton, C. W. I. Douglas, J. Mater. Sci. Mater. Med. 1995, 6, 695 – 698.
- [71] K. C. Dee, C. Ruecker, T. T. Andersen, R. Bizios, Biomaterials 1995, 17, 209 215.
- [72] C. A. van Blitterswijk, D. Bakker, S. C. Hesseling, H. K. Koerten, *Biomaterials* 1991, 12, 187 193.
- [73] R. Urlaub, U. Posset, R. Thull, J. Non-Cryst. Solids 2000, 265, 276– 284
- [74] U. Schubert, S. Tewinkel, F. Möller, Inorg. Chem. 1995, 34, 995 997.
- [75] E. Vogel, P. Meuer, W. Kiefer, R. Urlaub, R. Thull, J. Mol. Struct. 1999, 482 483, 241 – 245.
- [76] J. Popp, P. Rösch, E. Vogel, W. Kiefer in *Progress in Surface Raman Spectroscopy—Theory, Techniques and Application*, (Eds.: Z. Q. Tian, B. Ren), Xiamen University Press, Xiamen, 2000, pp. 163 166.
- [77] M. Schnitzer, S. U. Khan, Humic Substances in the Environment, Dekker, New York, NY, 1972.
- [78] P. Warwick, T. Hall, D. Read, Radiochim. Acta 1996, 73, 11 19.
- [79] Y. Yang, H. A. Chase, Spectrosc. Lett. 1998, 21, 821 848.
- [80] K. Nakamoto, Infrared and Raman Spectra of Inorganic and Coordination Compounds, Wiley, New York, NY, 1977.
- [81] E. Vogel, R. Gessner, M. H. B. Hayes, W. Kiefer, J. Mol. Struct. 1999, 482 483, 195 – 199.
- [82] J. Popp, W. Kiefer in Encyclopedia of Analytical Chemistry, Vol. 21 (Ed.: R. A. Mayer), John Wiley & Sons, New York, NY, 2000, pp. 13104 13143.
- [83] G. Bringmann, F. Pokorny in *The Alkaloids, Vol. 46* (Ed.: G. A. Cordell), Academic Press, New York, NY, 1995, pp. 127 – 271.
- [84] E. Urlaub, J. Popp, W. Kiefer, G. Bringmann, D. Koppler, H. Schneider, U. Zimmermann, B. Schrader, Biospectroscopy 1998, 4, 113 120.
- [85] P. Rösch, J. Popp, W. Kiefer, J. Mol. Struct. 1999, 480-481, 121-124.
- [86] P. Rösch, J. Popp, W. Kiefer, M. Grünsfelder, F.-C. Czygan in Spectroscopy of Biological Molecules: New Directions (Eds.: J. Greve, G. J. Puppels, C. Otto), Kluwer, London, 1999, pp. 583 – 584.
- [87] P. Rösch, W. Kiefer, J. Popp, Biopolymers 2002, 67, 358-361.
- [88] K. R. Beebe, R. J. Pell, M. B. Seasholtz, Chemometrics: A Practical Guide, Wiley & Sons, New York, NY, 1998.
- [89] Bruker Analytik GmbH, OPUS-NT Manual, Vers. 3, Ettlingen, 2000.
- [90] H. Schulz, H. H. Dres, R. Quilitzsch, H. Kruger, J. Near Infrared Spectrosc. 1998, 6, A125 – A130.
- [91] H. Schulz, B. Schrader, R. Quilitzsch, B. Steuer, Appl. Spectrosc. 2002, 56, 117 – 124.
- [92] D. Ivnitski, I. Abdel-Hamid, P. Atanasov, E. Wilkins, *Biosens. Bioelectron.* 1999, 14, 599 – 624.
- [93] D. Naumann, D. Helm, H. Labischinski, Nature 1991, 351, 81 82.
- [94] D. Naumann, S. Keller, D. Helm, C. Schultz, B. Schrader, H. Labischinski, J. Mol. Struct. 1995, 347, 399 – 405.
- [95] D. Naumann in *Practical Spectroscopy*, Vol. 24 (Eds.: H. U. Gremlich, B. Yan), Dekker, New York, NY, 2001, pp. 323 378.
- [96] D. Naumann, D. Helm, H. Labischinski, P. Giesbrecht in Modern Techniques for Rapid Micribiological Analysis (Ed.: W. H. Nelson), VCH, New York, NY, 1991, pp. 43 – 96.
- [97] K. Maquelin, L. P. Choo-Smith, T. van Vreeswijk, H. P. Endtz, B. Smith, R. Bennett, H. A. Bruining, G. J. Puppels, Anal. Chem. 2000, 72, 12 19.
- [98] H. C. van der Mei, D. Naumann, H. J. Busscher, *Infrared Phys. Technol.* 1996, 37, 561 – 564.
- [99] A. M. Melin, A. Perromat, G. Deleris, Appl. Spectrosc. 2001, 55, 23 28.
- [100] A. Fehrmann, M. Franz, A. Hoffmann, L. Rudzik, E. Wust, J. AOAC Int. 1995, 78, 1537 – 1542.
- [101] A. Fehrmann, M. Franz, A. Hoffmann, L. Rudzik, E. Wust, J. Mol. Struct. 1995. 348. 13 – 16.
- [102] D. Naumann, C.P. Schultz, D. Helm in Infrared Spectroscopy of Biomolecules, Wiley-Liss., New York, 1996, pp. 279 – 310.
- [103] R. Goodarce, E. M. Timmins, R. Burton, N. Kaderbhai, A. M. Woodward, D. B. Kell, P. J. Rooney, *Microbiology (Reading, U. K.)* 1998, 144, 1157 – 1170
- [104] R. Goodarce, R. Burton, N. Kaderbhai, E. M. Timmins, A. M. Woodward, P. J. Rooney, D. B. Kell, *NATO ASI Ser.*, Ser. 1 2000, 30, 111 – 136.
- [105] A. C. Williams, H. G. M. Edwards, J. Raman Spectrosc. 1994, 25, 673 677.

- [106] H. G. M. Edwards, N. C. Russell, R. Weinstein, A. C. Wynn-Williams, J. Raman Spectrosc. 1995, 26, 911–916.
- [107] S. Chada, W. H. Nelson, J. F. Sperry, Rev. Sci. Instrum. 1993, 64, 3088 3093.
- [108] W. H. Nelson, J. F. Sperry in Modern Techniques for Rapid Microbiological Analysis (Ed.: W. H. Nelson), VCH, New York, NY, 1991, pp. 97 – 142.
- [109] G. J. Puppels, F. F. M. de Mul, C. Otto, J. Greve, M. Robert-Nicoud, D. J. Arndt-Jovin, T. M. Jovin, *Nature* **1990**, *347*, 301 – 303.
- [110] K. Maquelin, L.-P. Choo-Smith, T. van Vreeswijk, P. H. Endtz, B. Smith, R. Bennet, H. A. Bruining, G. J. Puppels, Anal. Chem. 2000, 72, 12–19
- [111] G. J. Puppels in *Fluorescent and Luminescent Probes for Biological Activity* (Ed.: W. T. Mason), Academic Press, London, **2000**, pp. 377 406.
- [112] K. C. Schuster, I. Reese, E. Urlaub, J. R. Gapes, B. Lendl, Anal. Chem. 2000, 72, 5529 – 5534.
- [113] R. Gessner, P. Rösch, W. Kiefer, J. Popp, *Biopolymers* **2002**, *67*, 327 330.
- [114] R. Stöckle, C. Fokas, V. Deckert, R. Zenobi, B. Sick, B. Hecht, U. Wild, Appl. Phys. Lett. 1999, 75, 160 – 162.
- [115] C. Arcangeli, S. Cannistraro, *Biopolymers* **2000**, *50*, 179 186.

Received: August 23, 2001 [A 293] Revised: September 19, 2002